



## Mechanically Alloyed: Synthesis of Nanostructured Intermetallic Compound of Zinc Selenide

Ahmed A. Al-Joubori<sup>1</sup>, Affaan Uthman Moosa<sup>1</sup>, Mohanad Kadhim Mejbel<sup>1\*</sup>

Middle Technical University, Technical Engineering College-Baghdad, 10001 Baghdad, Iraq

Corresponding Author Email: [Mohanad@mtu.edu.iq](mailto:Mohanad@mtu.edu.iq)

<https://doi.org/10.18280/rcma.330107>

### ABSTRACT

**Received:** 16 December 2022

**Accepted:** 6 February 2023

#### Keywords:

*mechanical alloying, zinc selenide, thermal stability, intermetallic compound, X-ray diffraction*

In a high-energy SPEX 8000 shaker mill, the process of mechanical alloying (MA) was carried out on blended elemental Se and Zn powder blends. The resulting mixtures corresponded to the stoichiometric composition of Se-50 at. percent Zn. The generated phases' phase evolution was computed. In the early phases of milling, a supersaturated solid solution of Zn in Se generated. As the milling process progressed, the solid solubility grew, and after milling the powders for ten hours, it had achieved its maximum value of around 50 at. percent zinc. Milling the powders for 30 minutes resulted in the beginning of the formation of the zinc selenide phase, while milling the powders for 10 hours resulted in the formation of a homogenous zinc selenide phase. The thermal stability of zinc selenide was achieved by annealing this sample for one hour at a temperature of 1000°C. The findings demonstrate that nanocrystalline zinc selenide with high thermal stability may be produced by MA of pure Se and Zn powders, followed by annealing.

## 1. INTRODUCTION

Zinc selenide is a kind of binary semiconductor that falls within the category of group II-VI with a large band gap (2.45 eV) has attracted significant attraction in recent years because of its photo-optic properties [1, 2]. Since ZnSe has a wide band gap [3, 4], it is possible to be used as a substitute for CdS compound which is used in photovoltaic cells [5, 6]. Beside this application field, investigated application usage of the alloy ZnSe is short wavelength visible-light laser devices [7]. Earlier studies on semiconductor quantum dots have showed that it is essential to synthesis nano-crystallites size smaller than the excitation Bohr diameter which is about 9 nm to reach quantum size effects [8, 9]. Therefore, some techniques were developed to synthesize ZnSe nanoparticles which are stable at room temperature [10, 11]. However, the nanocrystal ZnSe can obtain by other methods such as molecular beam epitaxy method [12, 13], chemical vapor disposition method [14, 15], and hydrothermal method [16]. Producing the material by these methods is not only expensive but also controlling the size of nanoparticles is difficult.

Mechanical alloying is a powder processing method which has been described in details in this work [17, 18]. This processing method is a non-equilibrium solid state processing technique. During the process the powder particles faced an extreme plastic deformation in a ball mill with high energy. It is easily possible to produce nanostructured materials by mechanical alloying especially those whose elements have very high melting temperatures, making the utilization of fusion-based procedures challenging [19]. Moreover, in different times, the crystallite size is refined to nanometer structures and the lamellar spacing usually becomes small [17, 18]. Additionally, Achimovičová et al. [20] revealed that ZnSe

may be created by mechanically alloying powdered elements. The authors indicated the formation of cubic and hexagonal crystal structures ZnSe intermetallic compound during mechanical alloying synthesis. Moreover, they showed the hexagonal ZnSe phase disappears with extending the milling period due to the metastability of a hexagonal ZnSe phase. Motivated by the fact that MA produces nanocrystalline materials with lower energy consumption and in short times, intermetallic compound ZnSe was produced by a high energy ball mill.

## 2. EXPERIMENT

Selenium (99.99% purity and 88 $\mu$ m) and zinc powders (99.99% purity and 100 $\mu$ m) were blended to produce ZnSe compound according to the ZnSe phase diagram [21]. 10 grams of powder were mixed in a steel container in the proportion to 50 at. % Zn and Se accordingly. They were milled in (SPEX 8000) a high energy shaker mill up to 10 h. A process control agent PCA was used, around 2 wt. % of stearic acid, to limit the influence of excessive cold welding that occurs between the container walls and powder and also between the powder particles. In order to avoid powder contamination from the surrounding air, all handling of the powder took place inside of an argon-filled glove box. Heat treatment was done in ambient atmosphere at 1000°C for 1 hr with a heating rate of 5°C/min after the powder was milled for 10 hrs. In order to evaluate the microstructural changes that occurred during the mechanical alloying, at a 10 kV acceleration voltage, in a Zeiss Ultra 55 microscope, scanning electron microscopy (SEM) was performed. A Rigaku-DXR 3000 diffractometer was adopted to perform X-ray diffraction

(XRD) using CuK $\alpha$  radiation ( $\lambda=0.15418$  nm) 30 mA and at 40 kV settings. Diffraction patterns from 20° to 60° were recorded in the 2 $\theta$  range with a dwell time of 3 s and 0.05° step size. EDS was adopted in order to examine the milled powders chemical compositions and link them with the findings of the XRD experiment. Based on the success of synthesizing the ZnSe phase, this procedure has been subsequently extended to synthesize the Zn-50 at. % Se phases by milling zinc and selenium powders in the ratios of 50:50. However, in these particular instances, the relevant intermetallic were not capable of being directly produced by mechanical alloying; probably related to the ductile selenium being present in the powder mixture instead of the brittle ZnSe compound in the earlier investigation. Moreover, with an increase in the Ball to Powder Ratio (BPR), the amount of time needed to finish the reduction reaction became shorter.

### 3. RESULTS AND DISCUSSION

#### 3.1 XRD

When powders were milled for 15 mins ZnSe compound peaks could not be detected (Figure 1). Increasing the milling time to 30 mins causes almost complete alloying occurred as X-ray pattern agree with previous works. Further milling time up to 60 mins results in broadening of the ZnSe peaks which means that longer milling time deforms crystallinity of the material. Driving force for the solid-state reaction is attributed not only to heat mixing of elements, but also collisions of powders to steel balls. This collision causes fracture creating new surfaces and progressive increase in grain boundaries. Since grain boundaries are the energetic regions and surface area increases surface energy, particles may lower their energy by forming alloys.

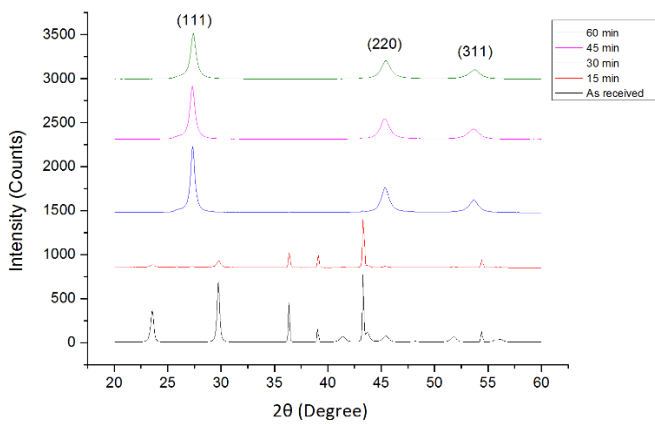


**Figure 1.** X-ray patterns of as received powder and 15, 30, 45, 60 min. milled powder

To see the effect of annealing on the crystal structure of milled powders, powders which were milled for 10 h were annealed at 1000°C for 1 hr. As seen in the Figure 2 no phase transformation occurred which means that the phase produced by MA is highly stable, but annealing results in sharpening of the peaks together with the formation of shoulders. Sharpening was expected due to increase in crystallinity as annealing occurs.

In order to compute the lattice strain and crystallite size, peak broadening was applied. This was done by measuring in radians the peak width  $B_0$ , at an intensity equal to half the

maximum value, which is termed the full width at half maximum (FWHM), and then applying the Williamson–Hall method [22, 23].

Crystallite size of powders was calculated by using Scherrer Equation [23]:

$$D = \frac{K \times \lambda}{B \times \cos(\theta)} \quad (1)$$

where,  $\lambda$ =Wavelength of the CuK $\alpha$  radiation,  $K$ =Shape factor (0.9), and  $D$ =Crystallite size.

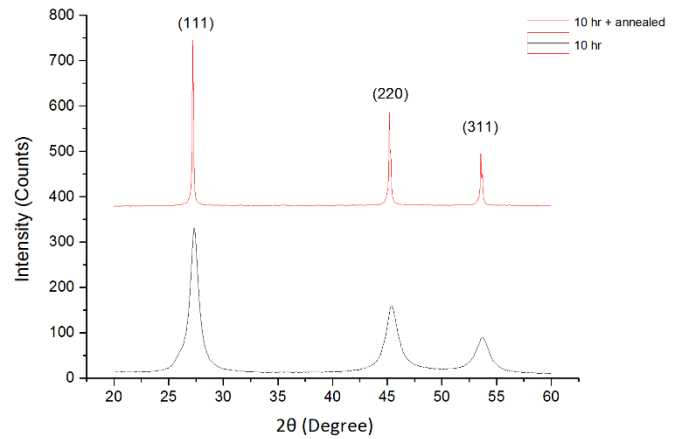


**Figure 2.** X-ray patterns of 10 hours milled and annealed powder

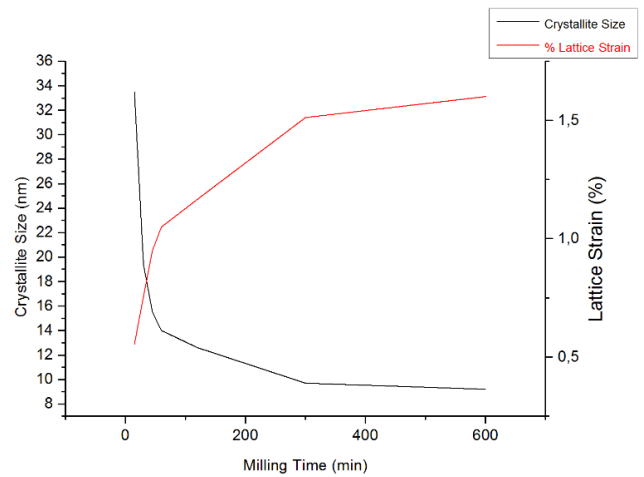


**Figure 3.** Calculated crystallite size and lattice strain during milling time

To get rid of the broadening coming from the instrument, the following formula was used.

$$B = [B_{measured}^2 - B_{instrumental}^2]^{0.5} \quad (2)$$

From the Figure 3, as milling time increases crystallite size decreases initially, but tends to saturate eventually which shows a logarithmic behavior. This is encouraging because in order to achieve quantum size effects, one must first create nanoscale crystallites with a size that is less than the excitation Bohr diameter (electron-hole pair), which is around 9 nm. This is why this development is so promising. Calculated crystallite size of the 10 hours milled powders which then annealed for 1 hour at 1000°C was 73.3 nm. This is an expected result since annealing causes ordering of atoms.

The lattice strain induced in milled powder due to distortion and structural defects was calculated using the formula given below [10]:

$$\varepsilon = \frac{B}{4 \times \tan(\theta)} \quad (3)$$

According to the Figure 3, lattice strain also shows a logarithmic behavior as milling time increase. The lattice strain of the sample milled for 15 min was 0.554%, whereas it was 1.601% after milling for 10 hours. To show the effect of annealing on the lattice strain behavior, the sample that was milled for 10 h and annealed for 1 h exhibited a strain of 0.201%.

### 3.2 SEM and EDS

Figures 4-9 shows microstructure and EDS analysis of blended and alloyed powders for various times. Figure 4 shows the blended Zn and Se powders before MA. While Se particles are generally <50 μm with angular shape, Zn particles are rounded and ligament shape with the size of <80 μm. Most of the Se particles appear <20 μm with irregular shape. However, there was no big difference in the Zn powder particles size. Initial powder size and hardness are very important for MA. The mean powder size after MA can range from 3 to 500 μm; this being a function of starting powder size distribution, composition and milling time.

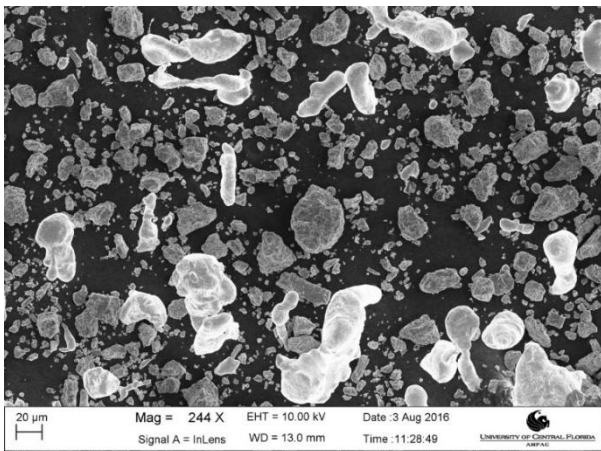


Figure 4. SEM micrograph showing Zn (white) and Se (grey) particles before milling

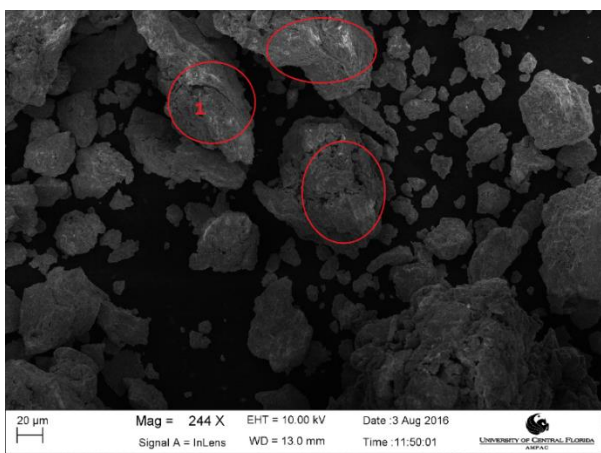


Figure 5. The appearance of Zn and Se powders after mechanical alloying for 15 min

The XRD result (Figure 1) showed that 15 minutes is not enough for the formation of ZnSe intermetallic compound. SEM result of 15 min milled powders also proved aforementioned claim (Figure 5). Nevertheless, partial MA was observed from the white regions which were marked as red circles. This means that elemental powders still exist in these marked areas. EDS analysis also supported this result where atomic percentage of Zn to Se is 16:84 at point 1 in the Figure 5. Moreover, the powder particles during milling are fractured, welded, flattened, and re-welded repeatedly. In the beginning of milling, the powder particles are tended to weld together. In addition, the size of the particles grows, with some becoming as much as three times larger than the particles that were there initially [16]. As seen in the Figure 5 partially alloyed powders are bigger in size comparing to as-blended powders (Figure 4) owing to over-welding in the beginning of alloying process. The particles get work-hardened when the mechanical milling process is repeated, and they break apart due to the brittle flake's fragmentation and/or by a fatigue failure mechanism as the process continues [16]. Figures 7 and 8 influence of milling time on the alloy formation and particle size. After 2 hours (Figure 7) more homogenous distribution of the particle size can be observed. This means that mechanical alloying process was done successfully. Furthermore, EDS analysis of 2 h milled powders show almost complete alloying composition where atomic percentage of Zn to Se is 58:42. Increasing the milling time to 10 h creates even more homogenous size distribution shown in the Figure 9. This would also result in more homogenous composition distribution of powders.

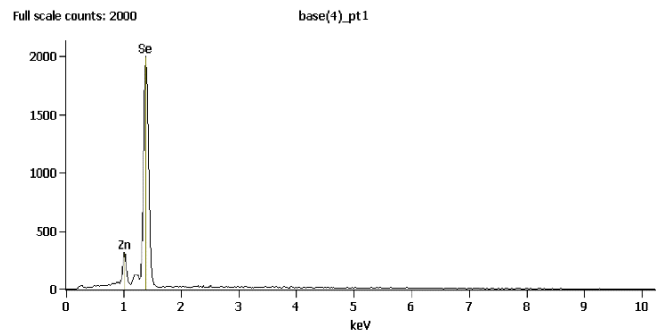


Figure 6. EDS result of milled powders for 15 min

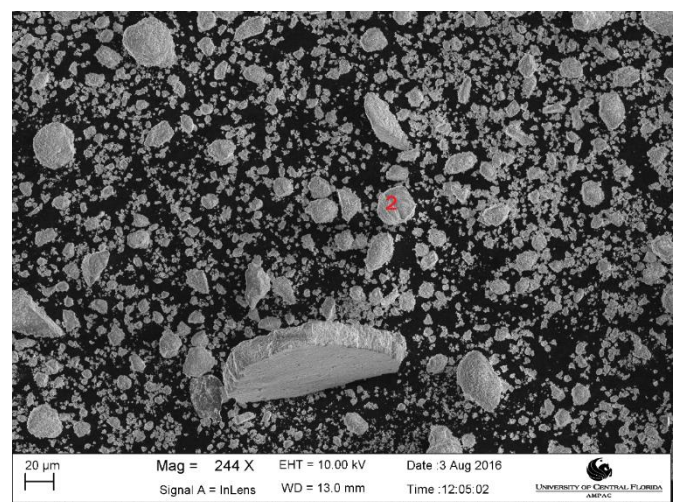
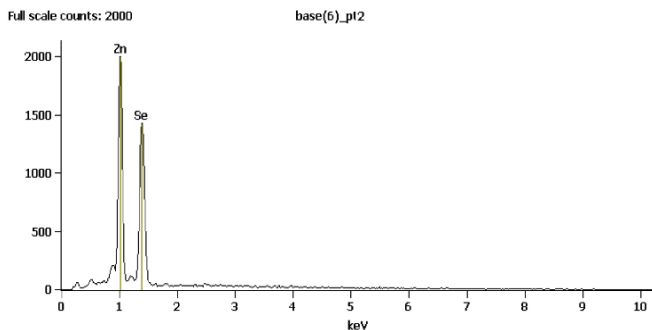
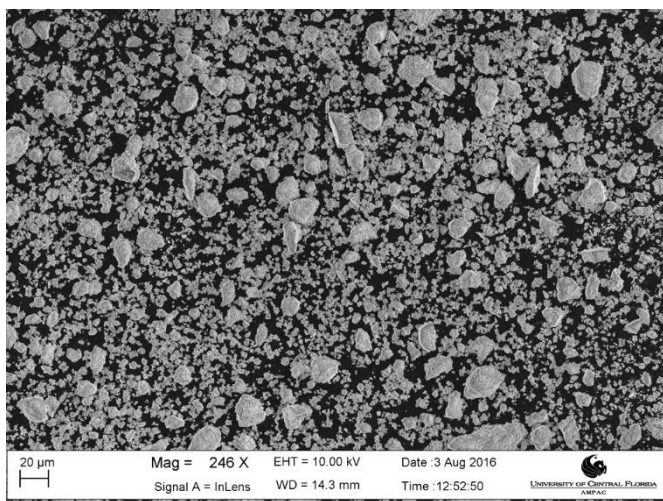


Figure 7. SEM micrograph of milled powders for 2 h



**Figure 8.** EDS result of milled powders for 2 hr taken from the X point in the Figure 7



**Figure 9.** SEM micrograph of milled powders for 10 h

#### 4. CONCLUSIONS

The mechanical alloying of nanocrystalline ZnSe intermetallic compound can be successfully synthesized beginning with elemental powders of pure zinc and selenium, having a composition of 50 percent zinc and 50 percent selenium. The research employing XRD and SEM methods revealed that an intermetallic compound of ZnSe is created within the first 15 minutes of milling. After 10 hours of milling, the powders were able to form a uniform ZnSe intermetallic compound. No phase transformation occurred after annealing the powder 1000°C for 1 hr which means that the phase produced by MA is highly stable.

#### REFERENCES

[1] Boldish, S.I., White, W.B. (1998). Optical band gaps of selected ternary sulfide minerals. *American Mineralogist*, 83(7-8): 865-871. <https://doi.org/10.2138/am-1998-7-818>

[2] Panda, S.K., Hickey, S.G., Demir, H.V., Eychmuller, A. (2011). Bright white-light emitting manganese and copper co-doped ZnSe quantum dots. *Angewandte Chemie International Edition*, 50(19): 4432-4436. <https://doi.org/10.1002/anie.201100464>

[3] Feng, B., Cao, J., Han, D., Yang, S., Yang, J. (2015). Study on growth mechanism and optical properties of ZnSe nanoparticles. *Journal of Materials Science:*

*Materials in Electronics*, 26: 3206-3214. <https://doi.org/10.1007/s10854-015-2818-5>

[4] Geng, J., Liu, B., Xu, L., Hu, F.N., Zhu, J.J. (2007). Facile route to Zn-based II–VI semiconductor spheres, hollow spheres, and core/shell nanocrystals and their optical properties. *Langmuir*, 23(20): 10286-10293. <https://doi.org/10.1021/la701299w>

[5] Murali, K.R., Dhanapandiyana, S., Manoharana, C. (2009). Pulse electrodeposited zinc selenide films and their characteristics. *Chalcogenide Letters*, 6(1): 51-56.

[6] Doña, J.M., Herrero, J. (1995). Chemical-bath deposition of ZnSe thin films: process and material characterization. *Journal of the Electrochemical Society*, 142(3): 764. <https://doi.org/10.1149/1.2048532>

[7] Leppert, V.J., Mahamuni, S., Kumbhojkar, N.R., Risbud, S.H. (1998). Structural and optical characteristics of ZnSe nanocrystals synthesized in the presence of a polymer capping agent. *Materials Science and Engineering: B*, 52(1): 89-92. [https://doi.org/10.1016/S0921-5107\(97\)00142-6](https://doi.org/10.1016/S0921-5107(97)00142-6)

[8] Che, J., Yao, X., Jian, H., Wang, M. (2004). Application and preparation of ZnSe nanometer powder by reduction process. *Ceramics International*, 30(7): 1935-1938. <https://doi.org/10.1016/j.ceramint.2003.12.190>

[9] Resch-Genger, U., Grabolle, M., Cavaliere-Jaricot, S., Nitschke, R., Nann, T. (2008). Quantum dots versus organic dyes as fluorescent labels. *Nature Methods*, 5(9): 763-775. <https://doi.org/10.1038/nmeth.1248>

[10] Li, G., Nogami, M. (1994). Preparation and optical properties of sol-gel derived ZnSe crystallites doped in glass films. *Journal of Applied Physics*, 75(8): 4276-4278. <https://doi.org/10.1063/1.355970>

[11] Wang, Y., Wang, M., Yao, X., Kong, F., Zhang, L. (2004). Nonlinear optical absorption of ZnSe nanocrystals embedded in silica glasses. *Journal of Crystal Growth*, 268(3-4): 575-579. <https://doi.org/10.1016/j.jcrysgro.2004.04.094>

[12] Gaines, J.M., Petruzzello, J., Greenberg, B. (1993). Structural properties of ZnSe films grown by migration enhanced epitaxy. *Journal of Applied Physics*, 73(6): 2835-2840. <https://doi.org/10.1063/1.353035>

[13] Ivanov, S.V., Toropov, A.A., Shubina, T.V., Sorokin, S.V., Lebedev, A.V., Sedova, I.V., Kop'ev, P.S., Gaines, J.M., Petruzzello, J., Monemar, B. (1998). Growth and excitonic properties of single fractional monolayer CdSe/ZnSe structures. *Journal of Applied Physics*, 83(6): 3168-3171. <https://doi.org/10.1063/1.367130>

[14] Hartmann, H., Hildisch, L., Krause, E., Möhling, W. (1991). Morphological stability and crystal structure of CVD-grown zinc selenide. *Journal of Materials Science*, 26: 4917-4923. <https://doi.org/10.1007/BF00549871>

[15] Rzepka, E., Roger, J.P., Lemasson, P., Triboulet, R. (1999). Optical transmission of ZnSe crystals grown by solid phase recrystallization. *Journal of Crystal Growth*, 197(3): 480-484. [https://doi.org/10.1016/S0022-0248\(98\)00773-8](https://doi.org/10.1016/S0022-0248(98)00773-8)

[16] Peng, Q., Dong, Y., Deng, Z., Sun, X., Li, Y. (2001). Low-Temperature elemental-direct-reaction route to II–VI semiconductor nanocrystalline ZnSe and CdSe. *Inorganic Chemistry*, 40(16): 3840-3841. <https://doi.org/10.1021/ic010042a>

[17] Suryanarayana, C. (2004). *Mechanical Alloying And Milling* (1st ed.). CRC Press. <https://doi.org/10.1201/9780203020647>

- [18] Suryanarayana, C. (2001). Mechanical alloying and milling. *Progress in Materials Science*, 46(1-2): 1-184. [https://doi.org/10.1016/S0079-6425\(99\)00010-9](https://doi.org/10.1016/S0079-6425(99)00010-9)
- [19] De Lima, J.C., Dos Santos, V.H.F., Grandi, T.A. (1999). Structural study of the Zn-Se system by ball milling technique. *Nanostructured Materials*, 11(1): 51-57. [https://doi.org/10.1016/S0965-9773\(98\)00161-5](https://doi.org/10.1016/S0965-9773(98)00161-5)
- [20] Achimovičová, M., Baláž, P., Ohtani, T., Kostova, N., Tyuliev, G., Feldhoff, A., Šepelák, V. (2011). Characterization of mechanochemically synthesized ZnSe in a laboratory and an industrial mill. *Solid State Ionics*, 192(1): 632-637. <https://doi.org/10.1016/j.ssi.2010.07.009>
- [21] Okamoto, H., Schlesinger, M.E., Mueller, E.M. (Eds.). (2016). *Alloy Phase Diagrams*. ASM International. <https://doi.org/10.31399/asm.hb.v03.9781627081634>
- [22] C. Suryanarayana and M. G. Norton, "X-Rays and Diffraction BT - X-Ray Diffraction: A Practical Approach," C. Suryanarayana and M. G. Norton, Eds. Boston, MA: Springer US, 1998, pp. 3-19. [https://doi.org/10.1007/978-1-4899-0148-4\\_1](https://doi.org/10.1007/978-1-4899-0148-4_1)
- [23] Cullity, B.D., Stock, S.R. (2001). *Elements of X-ray Diffraction*. 3rd ed. New York: Prentice-Hall.